Pergamon

Chemical Engineering Science, Vol. 51, No. 8, pp. 1333–1342, 1996

0009–2509/96 $15.00 + 0.00

0009–2509(95)00355–X

ON THE SOLUTION OF POPULATION BALANCE EQUATIONS BY DISCRETIZATION—II. A MOVING PIVOT TECHNIQUE

SANJEEV KUMAR and D. RAMKRISHNA*
School of Chemical Engineering, Purdue University, West Lafayette, IN 47907, U.S.A.

(*First received* 5 *May* 1995; *accepted* 17 *September* 1995)

Abstract—Discretized population balances of aggregating systems are known to consistently over-predict number densities for the largest particles. This over-prediction has been attributed recently by the authors (Kumar and Ramkrishna, 1996, *Chem. Engng Sci.* **51**, 1311–1332) to steeply non-linear gradients in the number density when a fixed pivotal particle size is used for each discrete interval. The present work formulates macroscopic balances of populations with due regard to the evolving non-uniformity of the size distribution in each size interval as a result of breakage and aggregation events. This is accomplished through a varying pivotal size for each interval adapting to the prevailing non-uniformity of the number density in the interval. The technique applies to a general grid and preserves any two arbitrarily chosen properties of the population. Comparisons of the numerical and analytical results have been made for pure aggregation for the constant, sum and product kernels. It is established that numerical predictions from macroscopic balances are significantly improved by an adapting pivot accounting for non-uniformities in the number density.

1. INTRODUCTION

In a recent paper (Part I) Kumar and Ramkrishna (1996) have proposed a fresh perspective on discretization methods for the solution of population balance equations. From this perspective, discretization is not viewed as an attempt to approximate the continuous number density function on a suitably fine scale. Rather, the salient feature of this new perspective is to target calculation of properties of the population of specific interest to an application without seeking the complete number density function. The properties concerned may be specific moments of the population, or more generally those that can be calculated from the number density function such as

$$F_i(t) = \int_0^\infty f_i(x) n(x,t)\,dx, \quad i = 1, 2, \ldots \tag{1}$$

and approximation of their distributions among the discrete particle size intervals

$$F_{i,k}(t) = \int_{v_k}^{v_{k+1}} f_i(x) n(x,t)\,dx, \quad i = 1, 2, \ldots \tag{2}$$

where v represents, say, particle volume. If the number density is known accurately over a fine enough size scale *all* such properties can be calculated accurately. However, often for engineering applications only specific properties may be of interest so that the precise evaluation of the number density function may be forsaken in favor of a more targeted calculation by using coarse discretization methods. The perspective of Kumar and Ramkrishna (1996) is one of specifically *designing* the discrete formulation for calculation of selected properties. This approach is of particular significance to model-based control of particulate systems in which there is considerable recent interest (Semino and Ray, 1995).

The essence of the technique of Kumar and Ramkrishna (1996) lies in effecting what the authors refer to as *preservation* of changes in the chosen properties resulting from particle break-up and/or aggregation. More precisely, there must be *consistency* between two different ways in which discrete equations for the properties of specific interest may be obtained. One is to discretize the continuous equation for the property derived from the continuous population balance equation. The other is to drive it from the discrete population balance equations. This consistency is enforced by appropriately apportioning the total property for a particle to the adjacent representative sizes.

This numerical technique (to be called Part I) has been tested for a large number of cases including polymerization–depolymerization and direct prediction of the second moment of the size distribution. The numerical predictions for all cases studied in Part I agree well with the analytical solutions with one exception. The use of a coarse geometric grid for solving PBEs with aggregation results in a consistent over-prediction in a size range that contains steeply decreasing number density (called "front"). Such over-prediction is a feature of other techniques proposed in the past as well, e.g. Bleck (1970), Gelbard *et al.* (1980), Hounslow *et al.* (1988).

* Corresponding author. Tel: 317-494-4066. Fax: 317-494-0805. email: ramkrish@ecn.purdue.edu.

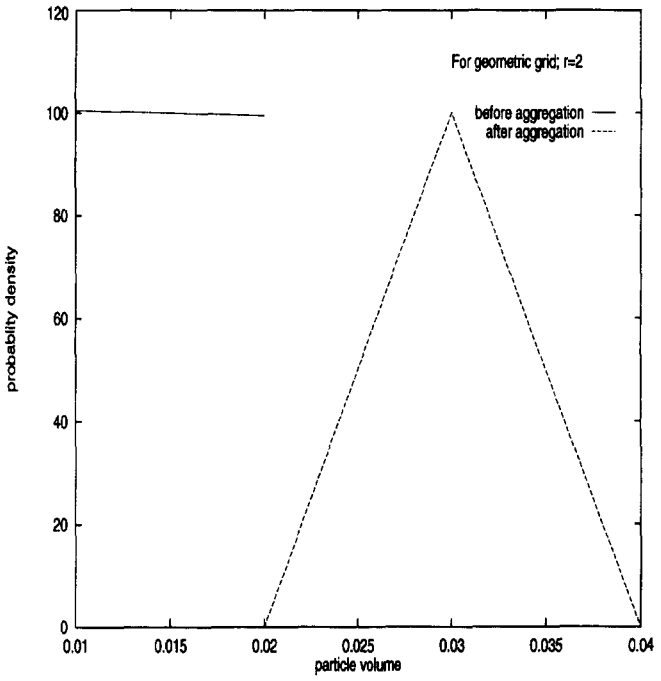

Fig. 1. Distribution of particles before and after aggregation (constant kernel), when particles are initially distributed uniformly.

In Part I, we have shown through a simple example that the over-predictions are due to the inadequacy of the uniform number density approximation to represent a steeply decreasing number density for aggregation. This example is reproduced here to provide the necessary motivation for the present work. Consider aggregation of particles for the constant kernel, with an initial population given as $n(v,0) = [(1/v_0)\exp(-v/v_0)]$. Let us focus on just a simple event—aggregation of particles in size range $\{v_i, 2v_i\}$ to form particles in size range $\{2v_i, 4v_i\}$ while ignoring all other possible interactions that can influence populations in the two size ranges considered. The number density of new particles in size range $\{2v_i, 4v_i\}$ and of those remaining in size range $\{v_i, 2v_i\}$ at time t can be easily calculated. The number densities for both the size ranges can be scaled separately to obtain the corresponding probability densities (which do not depend on time for the constant kernel). Figure 1 shows a plot of these densities for $v_i \ll v_0$. The same densities for $v_i \gg v_0$ are plotted in Fig. 2. As expected, the figures show that the distribution of new particles in size range $\{2v_i, 4v_i\}$ depends on the distribution of the aggregating particles in size range $\{v_i, 2v_i\}$.

In comparison, the discretization technique of Part I equates this process to the aggregation of N_i particles of size x_i, a representative size for size range $\{v_i, 2v_i\}$, form $N_i/2$ particles of size $2x_i$, irrespective of the distribution of particles in size range $\{v_i, 2v_i\}$. Figure 1 shows that this is a good representation for number densities that do not vary steeply. For those varying steeply, such as the one shown in Fig. 2, most of the new particles that are formed at any time t lie near the lower boundary of the size range $\{2v_i, 4v_i\}$. The discrete representation, however, advances the new $N_i/2$ particles to the middle of the size range. More importantly, for size-dependent coalescence kernels, the aggregation process is carried out at frequency $q(x_i, x_i)$, rather than a more relevant frequency $[\sim q(v_i, v_i)]$ that corresponds to the most populated sizes in size range $\{v_i, 2v_i\}$.

There are two ways to improve the accuracy of the numerical solution: (i) choose smaller sections such that the number density does not vary significantly over a section width; (ii) develop a technique that accounts for the variation of number density in a size range. The former has already been demonstrated in Part I with several strategies such as total or selective refining of the grid; the latter is the focus of the present work. The technique proposed here has the advantage over (i) in that it can be used with a coarse grid. It does away with a fixed representative (pivot) of each size interval which does not adapt efficiently to sharp variations in the number density and replaces it by a "moving" pivot.

2. A MOVING PIVOT TECHNIQUE

A complete description of the evolution of a population due to the particulate processes is provided through a density function which can then be used to obtain all evolutionary properties associated with the population. However, specific applications require only selected properties associated with a size

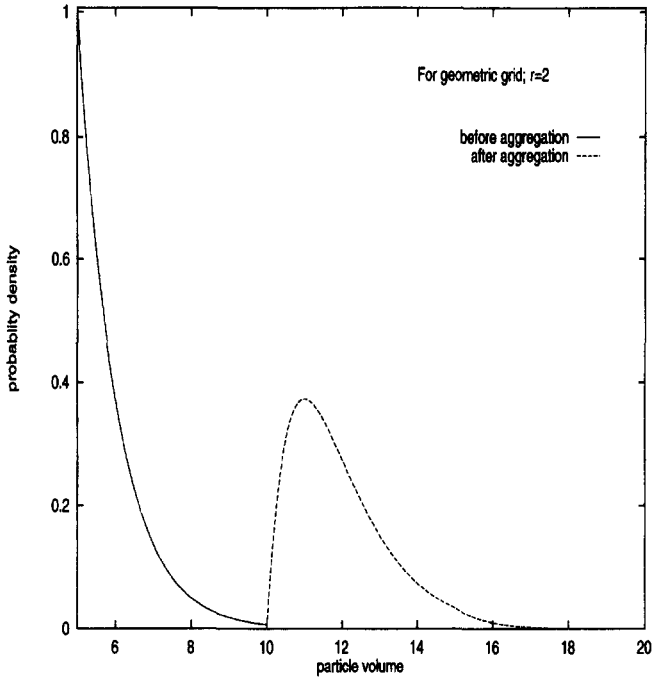

Fig. 2. Distribution of particles before and after aggregation (constant kernel), when particles are initially distributed exponentially.

distribution. As noted in Part I, macroscopic balances (discretization techniques) can be designed to obtain with minimum effort the desired information associated with a size distribution accurately, while relaxing on other less important properties. This is best accomplished if we solve directly for the quantities of interest, as illustrated in Part I.

The macroscopic balances that consider the interaction of a sub-population of particles in a size range with other sub-populations (for other size ranges) have their limitations as shown by the example in the previous section. Similar limitations also exist when the number density in a size range is assumed to be uniform as evidenced by the numerical results of Bleck (1970) and Gelbard and Seinfeld (1980). In analogy with transport processes (integral momentum balances for boundary layers), the macroscopic balances can be made more accurate by incorporating pertinent details of the variation of number density within a size range (This is akin to the classical approximation of the velocity profile in a boundary layer in von Karman's integral momentum balances.) The distinguishing feature of the technique presented here is therefore the recognition of the variation of number density with size in a size range and its evolution with time due to particle break-up and aggregation.

Clearly, an accurate representation of this variation requires complete knowledge of the number density, which macroscopic balances cannot afford. In this work, we will therefore include the variation of number density in a simple and an approximate way (e.g. using approximate forms of the velocity profile in integral momentum balances).

We propose that if the properties of interest associated with a size distribution are $p(v)$ and $u(v)$ $[\equiv p(v)g(v)]$, then for their direct prediction, a section i (size range v_i to v_{i+1}) should be identified with two quantities, $P_i(t)$ defined as

$$P_i(t) = \int_{v_i}^{v_{i+1}} p(v)n(v,t)\,dv \tag{3}$$

and a pivot $x_i(t)$ defined as

$$\int_{v_i}^{v_{i+1}} u(v)n(v,t)\,dv = \int_{v_i}^{v_{i+1}} g(v)p(v)n(v,t)\,dv = g[x_i(t)]P_i(t). \tag{4}$$

The definition of $x_i(t)$ has been chosen such that its location in size range $\{v_i, v_{i+1}\}$ reflects the variation of the relevant density $u(v)n(v,t)$ in the ith size range. It also allows for the estimation of property $u(v)$ for the ith section directly from $P_i(t)$ and $x_i(t)$. For the type of density shown in Fig. 1, x_i stays closer to the middle of the section and for steeply decreasing densities, as shown in Fig. 2, it stays closer to the lower end of the section, i.e. closer to v_i, thus capturing the aggregation process more realistically. If the density in a section changes from steeply decreasing to nearly uniform due to the particulate process, the pivot moves from the lower end of the section to the middle. Thus, the location of the pivot in a section at any instant reflects the variation of the relevant density in that size range. If proper equations are obtained for

the movement of the pivot with time, a change in the position of the pivot will appropriately reflect the changing density distribution for the section. The rest of this section is devoted to the derivation of the new discrete equations for directly obtaining the quantities of interest and the movement of the pivot. Note also that a moving pivot is more in keeping with the dictates of the mean value theorem of the calculus.

2.1. *Derivation of the discrete equations*

Let us begin with the equation for number balances when particles breakup and aggregate.

$$\frac{\partial n(v,t)}{\partial t} = \tfrac{1}{2}\int_0^v n(v-v',t)n(v',t)q(v-v',v')\,\mathrm{d}v' - \int_0^\infty n(v,t)n(v',t)q(v,v')\,\mathrm{d}v' - \Gamma(v)n(v,t) + \int_v^\infty \beta(v,v')\Gamma(v')n(v',t)\,\mathrm{d}v'. \tag{5}$$

For the quantity of interest $p(v)$, eq. (5) can be transformed to

$$\frac{\partial \tilde{p}(v,t)}{\partial t} = \tfrac{1}{2}p(v)\int_0^v \tilde{p}(v-v',t)\tilde{p}(v',t)r(v-v',v')\,\mathrm{d}v' - \tilde{p}(v,t)p(v)\int_0^\infty \tilde{p}(v',t)r(v,v')\,\mathrm{d}v' - \Gamma(v)\tilde{p}(v,t) + \int_v^\infty \left[\frac{p(v)}{p(v')}\right]\beta(v,v')\Gamma(v')\tilde{p}(v',t)\,\mathrm{d}v' \tag{6}$$

where

$$\tilde{p}(v,t) = p(v)n(v,t) \tag{7}$$

$$r(v,v') = q(v,v')/[p(v)p(v')]. \tag{8}$$

An equation for the variable $P_i(t)$, as defined earlier in eq. (3), can be obtained by integrating eq. (6) from v_i to v_{i+1}. Thus,

$$\frac{\mathrm{d}P_i(t)}{\mathrm{d}t} = \tfrac{1}{2}\int_{v_i}^{v_{i+1}} P(v)\,\mathrm{d}v \times \int_0^v \tilde{p}(v-v',t)\tilde{p}(v',t)r(v-v',v')\,\mathrm{d}v' - \int_{v_i}^{v_{i+1}} \mathrm{d}v\,\tilde{p}(v,t)p(v)\int_0^\infty \tilde{p}(v',t)r(v,v')\,\mathrm{d}v' - \int_{v_i}^{v_{i+1}} \mathrm{d}v\,\Gamma(v)\tilde{p}(v,t) + \int_{v_i}^{v_{i+1}} \mathrm{d}v \times \int_v^\infty \left[\frac{p(v)}{p(v')}\right]\beta(v,v')\Gamma(v')\tilde{p}(v',t)\,\mathrm{d}v'. \tag{9}$$

Identical equations can be obtained for all $P_j(t)$'s and thus eq. (9) can be considered as a set of equations for $i = 1, 2, \ldots, M$ where M is the total number of sections.

We now express the density $p(v,t)$ in terms of variables P_j's and x_j's (explicit dependence on t is suppressed for convenience) as

$$p(v,t) = \sum_i P_i\delta(v - x_i). \tag{10}$$

Substituting for $p(v,t)$ from eq. (10) in eq. (9), we obtain

$$\frac{\mathrm{d}P_i}{\mathrm{d}t} = \sum_{\substack{j,k \\ v_i \leqslant (x_j+x_k) < v_{i+1}}}^{j\geqslant k} [1 - \tfrac{1}{2}\delta_{j,k}]p(x_j+x_k)r_{x_j,x_k}P_jP_k - p(x_i)P_i\sum_{k=1}^{M} r_{x_i,x_k}P_k + \sum_{j\geqslant i}\Gamma(x_j)P_j\frac{\bar{B}_{i,j}^{(p)}}{p(x_j)} - \Gamma(x_i)P_i. \tag{11}$$

Here

$$\bar{B}_{i,j}^{(s)} = \int_{v_i}^{v_{i+1}} s(v)\beta(v,x_j)\,\mathrm{d}v \tag{12}$$

$$\beta(v,x_k) = 0, \quad v > x_k. \tag{13}$$

The equation for the movement of pivot x_i with time can be obtained in the following manner. We first derive an equation for quantity $\int_{v_i}^{v_{i+1}} u(v)n(v,t)\,\mathrm{d}v$, which is easily obtained by multiplying eq. (6) with $g(v)$ and then integrating it from v_i to v_{i+1}. Thus,

$$\frac{\mathrm{d}}{\mathrm{d}t}\left[\int_{v_i}^{v_{i+1}} g(v)p(v,t)\,\mathrm{d}v\right] = \tfrac{1}{2}\int_{v_i}^{v_{i+1}} u(v)\,\mathrm{d}v\int_0^v \tilde{p}(v-v',t)\tilde{p}(v',t)r(v-v',v')\,\mathrm{d}v' - \int_{v_i}^{v_{i+1}}\mathrm{d}v\,\tilde{p}(v,t)u(v)\int_0^\infty \tilde{p}(v',t)r(v,v')\,\mathrm{d}v' + \int_{v_i}^{v_{i+1}}\mathrm{d}v\int_0^\infty \frac{u(v)}{p(v)}\beta(v,v')\Gamma(v')\tilde{p}(v',t)\,\mathrm{d}v' - \int_{v_i}^{v_{i+1}}\mathrm{d}v\,g(v)\Gamma(v)\tilde{p}(v,t). \tag{14}$$

Introducing eq. (4) on the l.h.s. and differentiating x_iP_i w.r.t. time, we obtain

$$P_i\frac{\mathrm{d}g(x_i)}{\mathrm{d}t} + g(x_i)\frac{\mathrm{d}P_i}{\mathrm{d}t} = \text{r.h.s. of eq. (14)}. \tag{15}$$

Substituting for $\tilde{p}(v,t)$ from eq. (10) and for $\mathrm{d}P_i/\mathrm{d}t$ from eq. (11), the final equation for the variation of $g(x_i)$ can be shown to be

$$\frac{\mathrm{d}g(x_i)}{\mathrm{d}t} = \frac{1}{P_i}\sum_{\substack{j,k \\ v_i \leqslant (x_j+x_k) < v_{i+1}}}^{j\geqslant k} [1 - \tfrac{1}{2}\delta_{j,k}][u(x_j+x_k) - g(x_i)p(x_j+x_k)]r_{x_j,x_k}P_jP_k + \frac{1}{P_i}\sum_{j\geqslant i}\Gamma(x_j)P_j\left[\frac{\bar{B}_{i,j}^{(u)} - g(x_i)\bar{B}_{i,j}^{(p)}}{p(x_j)}\right]. \tag{16}$$

Coefficients $\bar{B}_{i,j}^{(u)}$ and $\bar{B}_{i,j}^{(p)}$ can be evaluated from equations similar to eq. (12).

Thus, the sets of equations in eq. (11) and eq. (16) complete the set of ordinary differential equations

that need to be solved simultaneously for a solution. It is emphasized here that the present technique retains the capacity of that in Part I to deal with multiple breakage and a general grid. Further, the final equations obtained here are internally consistent with the discrete equations for the evolutionary equations for $p(v)$ and $u(v)$ properties of the complete size distribution.

2.2 *Discrete equations for the preservation of numbers and mass*

For internal consistency with regard to zeroth $[p(v) = 1]$ and first moment $[u(v) = v]$ (total numbers and total mass respectively), sets of equations in eq. (12) and eq. (16) reduce to the following simple equations:

$$\frac{dN_i}{dt} = \sum_{\substack{j,k \\ v_i \leq (x_j + x_k) < v_{i+1}}}^{j \geq k} [1 - \tfrac{1}{2}\delta_{j,k}]\, q_{x_j, x_k} N_j N_k - N_i \sum_{k=1}^{M} q_{x_i, x_k} N_k + \sum_{j \geq i} \Gamma(x_j) N_j \bar{B}_{i,j}^{(1)} - \Gamma(x_i) N_i \tag{17}$$

$$\frac{dx_i}{dt} = \frac{1}{N_i} \sum_{\substack{j,k \\ v_i \leq (x_j + x_k) < v_{i+1}}}^{j \geq k} [1 - \tfrac{1}{2}\delta_{j,k}][(x_j + x_k) - x_i] q_{x_j, x_k} N_j N_k - \frac{1}{N_i} \sum_{j \geq i} \Gamma(x_j) N_j [\bar{B}_{i,j}^{(v)} - x_i \bar{B}_{i,j}^{(1)}] \tag{18}$$

where

$$\bar{B}_{i,j}^{(1)} = \int_{v_i}^{v_{i+1}} \beta(v, x_j)\, dv \qquad \bar{B}_{i,j}^{(v)} = \int_{v_i}^{v_{i+1}} v\beta(v, x_j)\, dv. \tag{19}$$

3. NUMERICAL RESULTS

The present moving pivot technique, like the fixed pivot technique of Part I, can be used for the prediction of the desired properties with a general grid (uniform, geometric or non-regular) for pure breakage, pure aggregation, polymerization–depolymerization (solution of discrete–continuous PBEs) and the prediction of higher moments. This distinguishing feature of the moving-pivot technique, however, is the inclusion of the addditional information in macroscopic balances on how the number density varies with particle size in various size ranges. The focus of the numerical results presented here is therefore on testing the present technique for its special features only, and not an exploration of its full potential (these issues are addressed in Part I). Also, the numerical results have not been compared with other techniques as the only discrete technique that addresses the variation of number density in a size range (Sastry and Gaschignard, 1981) involves a large number of double integrals and is very computation intensive.

As discussed earlier in the paper, the fixed pivot technique over-predicts the numerical results for pure aggregation in the size range that contains the front. The present technique was motivated by the viewpoint that this over-prediction could be remedied by including additional details in the macroscopic balances. In this section, we therefore present the new results only for pure aggregation problems and compare them with the analytical results and the numerical results obtained using the fixed pivot technique for the same grid.

The numerical results for the present technique have been obtained for the preservation of properties $p(v) = 1$ and $u(v) = v$, i.e. through the solution of eqs (17) and (18) and have been compared with the analytical solutions presented by Scott (1968). The numerical results have also been compared with those obtained with the fixed pivot technique for the same grid. The initial conditions for $N_i(t)$s and $x_i(t)$s for all calculations presented here correspond to the following number density distribution:

$$n(v, 0) = \frac{1}{v_0} \exp(-v/v_0). \tag{20}$$

The volume of the smallest particle considered in the calculations is 10^{-5}, 1000 times smaller than the initial average volume. The numerical results have been presented in terms of cumulative oversize numbers vs the particle volume, where the former is defined as

$$\mathrm{CON}(v, t) = \int_0^{\infty} n(v, t)\, dv. \tag{21}$$

Such a plot emphasizes the predictions for number density in the tail region and the zeroth moment of the size distribution (total numbers) in single plot.

Figure 3 shows the numerical and the analytical results for the constant kernel $q(v, v') = 1$ for degree of aggregation $N(t)/N(0) = 4 \times 10^{-3}$, where $N(t)$ is the total number of particles at time t. The numerical results presented here have been obtained for two geometric grids ($v_{i+1} = rv_i$) for $r = 2$, 1.4 (the numerical technique can, of course, be used with a general grid). The figure clearly shows that the fixed-pivot technique for $r = 2$ does not predict the shape and the movement of the front correctly; the total number of particles however, is predicted accurately as all the curves coincide with the analytical solution for $v \to 0$ [these results are the same as those would be obtained by the technique of Hounslow *et al.* (1988)]. The moving pivot technique with the same grid results in some under-prediction of the movement of the front (shape is predicted correctly), but in comparison with the results obtained with the fixed pivot technique, the present technique makes significantly improved predictions. This is quite clear from only 33% under-prediction for the moving pivot technique in comparison with 1800% over-prediction for the fixed pivot technique for the prediction of the particle size for $\mathrm{CON}(v, t) = 10^{-20}$.

With the use of a finer grid, $r = 1.4$, the results obtained by both the techniques are improved significantly; 16% under-prediction for the moving pivot

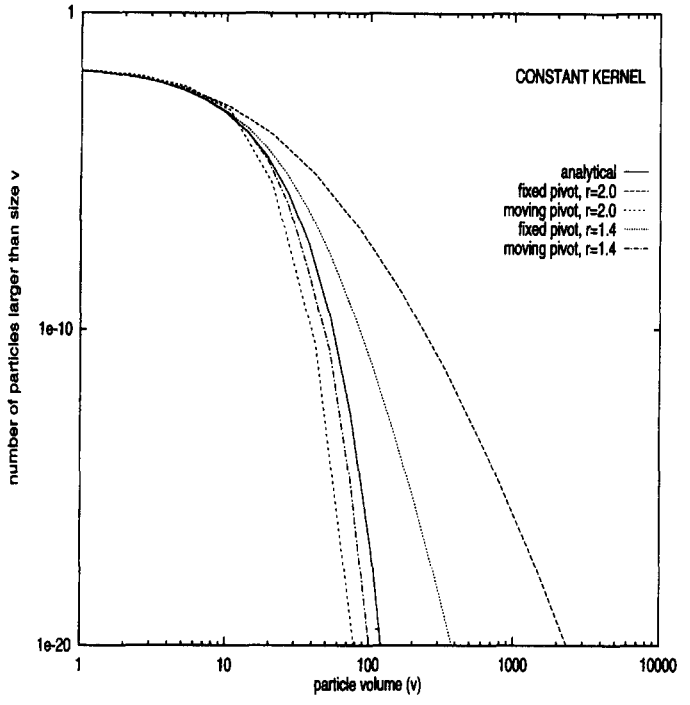

Fig. 3. A comparison of the numerical and the analytical size distributions for pure aggregation with the constant kernel $q(v,v') = 1$, at time $t = 100$, $N(t)/N(0) = 4 \times 10^{-3}$.

and 200% over-prediction for the fixed pivot for the prediction of the particle size for $\mathrm{CON}(v,t) = 10^{-20}$. As the grid is refined further, the numerical solutions for both the techniques approach the analytical solution. It is likely, though, that for extremely accurate predictions, both the techniques would require similar grids.

For size-dependent kernels, the fixed pivot technique makes poor predictions for the shape as well as the movement of the front. This is clearly shown in Figs 4 and 5 for the sum and the product kernels respectively. The extent of over-prediction with a geometric grid, $r = 1.5$, for particle volume v corresponding to the smallest value of $\mathrm{CON}(v,t)$ shown in these figures is approximately two orders of magnitude. In comparison, the moving pivot technique, with the same grid, under-predicts the same results just by a factor of 1.7. With a finer grid ($r = 1.2$), both techniques make improved predictions and as stated before, extremely accurate results may be obtained for similar grids only.

It should be pointed out here that both the techniques, irrespective of the type of grid employed, predict the total number of particles [CON(0)] correctly and conserve mass.

The numerical results for all the three kernels indicate that the inclusion of additional information in macroscopic balances significantly improves their ability to predict the correct results. By allowing the location of a pivot to correspond to more populated sizes in a size range initially as well as at all later times, the large over-prediction observed for the fixed pivot technique is changed to a slight under-prediction. A further improvement in the numerical predictions within the framework of discrete balances is indeed possible. However, the form of the first term on the r.h.s. of eq. (5) indicates that this is possible only through a more precise specification of the variation of number density with particle size. This, of course, increases the complexity of the numerical technique.

Recently, Kostoglou and Karabelas (1994) have compared the numerical techniques proposed by Gelbard and Seinfeld (1980), Batterham *et al.* (1981), Marchal *et al.* (1988) and Hounslow *et al.* (1988). Their findings indicate that the numerical technique proposed by Batterham *et al.* (1981) makes good predictions of the advancing front, even though it counts the aggregation of particles in the same size range twice and does not predict the total number of particles correctly. The new understanding brought out by the present work clearly indicates that this is due to a fortuitous cancellation of errors.

As with the technique proposed in Part I, the fixed pivot technique of Batterham *et al.* should result in over-prediction of the front. However, their strategy to assign a large fraction of new particles to the smaller pivot counterbalances the over-prediction. This, however, leads to wrong predictions of the total number of particles. [The authors assign $\frac{3}{4}$ particle to size x_i and $\frac{3}{8}$ to x_{i+1} when a particle of size $3x_i/2$ is formed. Similarly for other new particles ($x_i \leqslant v < 3x_i/2$), more than one, i.e. v/x_i, particle is assigned to x_i and none to x_{i+1}.]

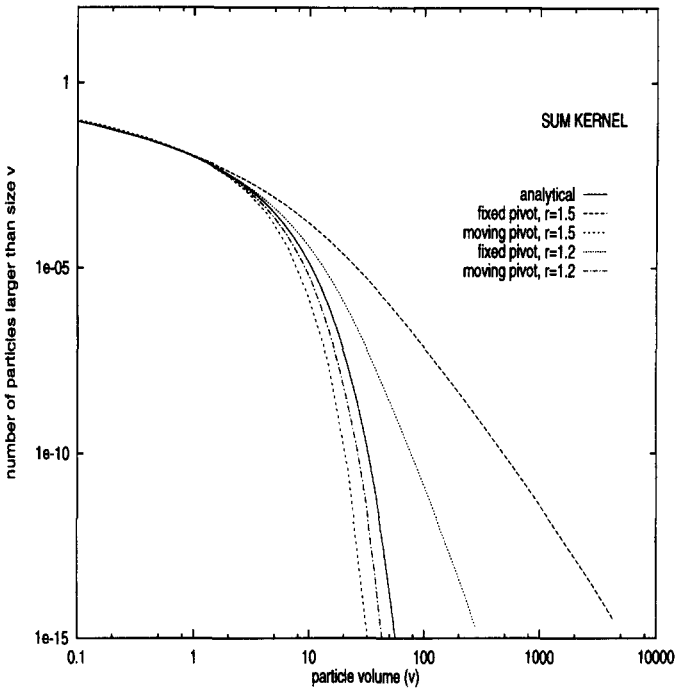

Fig. 4. A comparison of the numerical and the analytical size distributions for pure aggregation with sum kernel $q(v, v') = v + v'$, at time $t = 40$, $N(t)/N(0) = 0.135$.

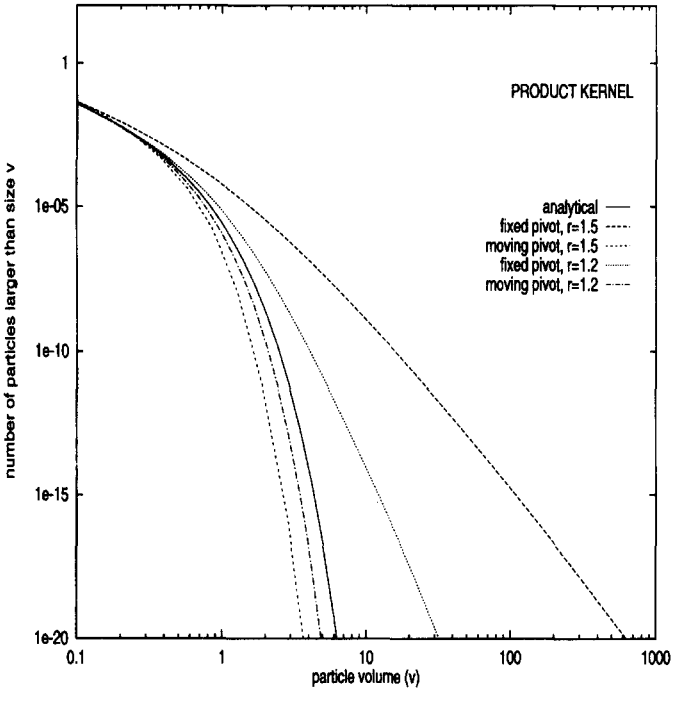

Fig. 5. A comparison of the numerical and the analytical size distributions (Scott, 1968) for pure aggregation with the product kernel $q(v, v') = vv'$, at time $t = 500$, $N(t)/N(0) = 0.875$.

3.1. *Choice of technique*

Kostoglou and Karabelas (1994) have compared the numerical techniques proposed before 1994. Their computations show that the technique proposed by Hounslow *et al.* (1988) is the best alternative. Since then, Hounslow's group (Litster *et al.*, 1995) has generalized original technique to a geometric grid of type $v_{i+1}/v_i = r$ for the preservation of numbers and mass. The parameter r is restricted to values $2^{1/q}$, where q is a positive integer. In this section, therefore, we will

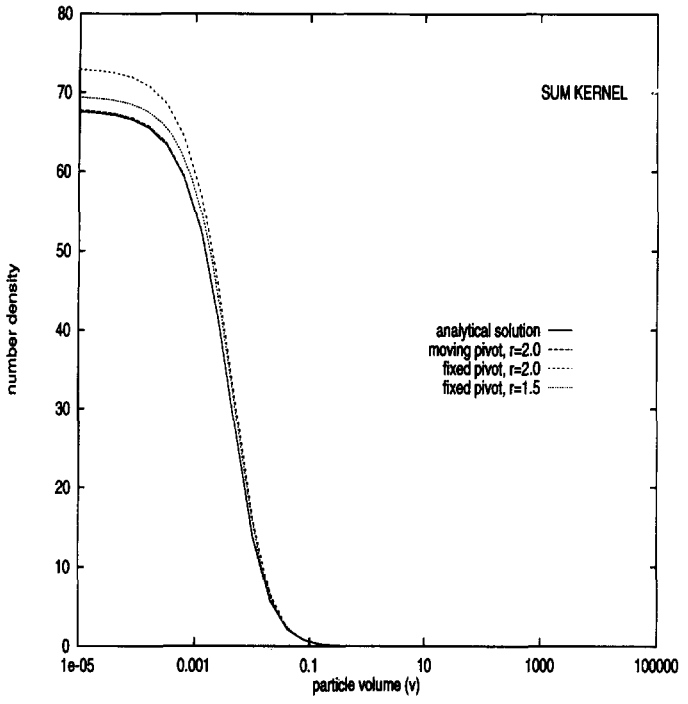

Fig. 6. A comparison of the numerical and the analytical number density distribution for pure aggregation with sum kernel for the same conditions as those in fig. 4 (semi-linear plot).

confine ourselves to the comparison of only three techniques—Litster *et al.* (1995), the fixed pivot of Part I and the moving pivot of the present work.

We begin with a comparison of the features of the fixed pivot technique and the technique of Lister *et al.* The former applies for all values of parameter r for geometric grid and also arbitrary grids (see Figs 13 and 16 of Part I), whereas the latter works only with selected geometric grids ($r = 2, \sqrt{2}, 2^{1/3}, \ldots$); the former can preserve general properties (see Figs 10 and 11 of Part I), whereas the latter is confined only to numbers and mass. The simplicity of the underlying concept in the fixed pivot technique, that the particles should be assigned to the adjoining pivots such that the two properties are preserved, naturally leads to discrete equations for pure breakage and simultaneous breakage and coalescence. Hill and Ng (1995), on the other hand, have followed Hounslow *et al.* to develop a discretization technique for pure breakage with the result that their technique has somewhat similar shortcomings. It can preserve numbers and mass only; furthermore, it suffers from the additional drawback that the coefficients of discretization depend on the breakage functions requiring elaborate derivations as demonstrated through their examples.

We have carried out computations for several cases using the fixed pivot and the technique of Litster *et al.* For identical grids and preservation of numbers and mass in the fixed pivot technique, the predictions made by both the techniques are exactly identical. The computation for both the techniques were carried out by using DIVPAG subroutine of IMSL with the same demands on the accuracy and they show that the fixed pivot technique takes less CPU time. As the number of equations used is increased, the fixed pivot technique becomes increasingly more efficient. This is also in agreement with our finding that the CPU time for the fixed pivot technique increases as q^2 whereas Litster *et al.* report that for their technique it increases as q^3. Thus, it is clear that the fixed pivot technique is a very powerful, general and computationally efficient technique, and for appropriate values of involved parameters it produces solutions which are exactly identical to those of Hounslow *et al.* and Litster *et al.* and takes less computation time.

We now compare the fixed pivot and the moving pivot techniques. To help us assess the effectiveness of the two techniques, we have re-plotted the results for the size-dependent sum kernel (Fig. 4) in terms of $n(v)$ vs v plot in Fig. 6 and extended $\log[n(v)]$ vs v plot in Fig. 7. These results indicate that in the small particle size range, the moving pivot technique makes very accurate predictions even with a coarse grid and these are better than those obtained by using the fixed pivot technique with twice as fine a grid. Figure 7 contains even more interesting results. It shows that the fixed pivot technique predicts a tail of type $v^{-\mu}$ rather than $\exp(-v/v_0)$ and as the grid is made finer, the predictions are improved but the non-exponential nature of the tail persists.

In comparison, the moving pivot technique makes near perfect predictions of the shape of the exponential tail even for $r = 2$; its location, however, is underpredicted and as shown earlier in Figs 3–5, the extent

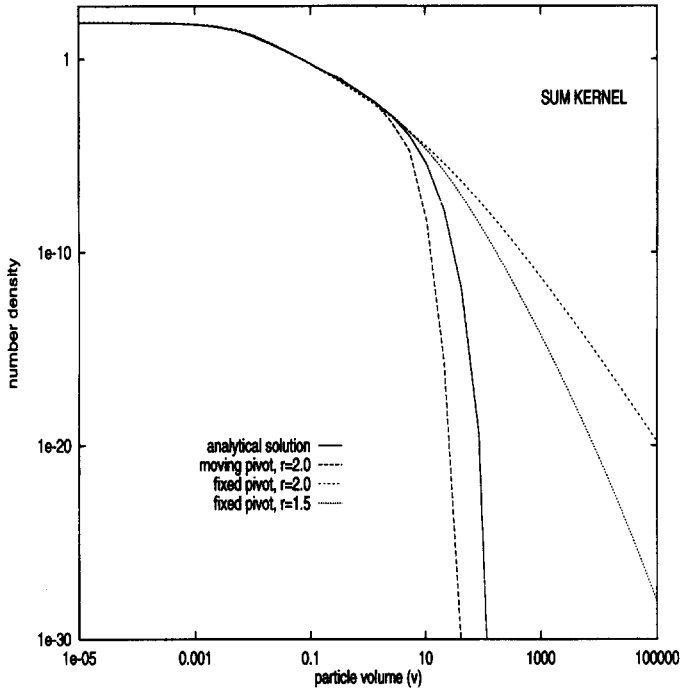

Fig. 7. Representation of the same information as in fig. 6 on an extended *log* – *log* scale.

of under-prediction can be reduced by choosing a suitable grid. Thus, accurate predictions of the populations of small particles and moments of the size distribution, and a near perfect prediction of the shape of the tail, all for coarse grids, are the advantages that only the moving pivot technique offers. Figures 6 and 7 show that the results obtained with the moving pivot for $r = 2$ are much better than those obtained for $r = 1.4$ for the fixed pivot. The number of equations employed in both the cases are the same; however, the former involves more computation time because the inequalities involved in eq. (11) need to be worked out repeatedly due to the evolving nature of the size distribution.

Thus, for the same number of equations, the difference in the CPU time for the time techniques is expected to be of the order of additional time needed for updating the inequalities. Our computation on a SUN Sparc station 5 indicate that for 60 equations, the fixed pivot and the moving-pivot techniques require 2 s and 14 s respectively; the time needed for updating the inequalities, however, is only 0.3 s. For the constant kernel, the corresponding times are 2 and 5 s and the time for updating the inequalities is mere 0.28 s. It therefore appears that much more than expected differences in the CPU times are due to inefficient implementation of the numerical technique. We are currently developing an ODE integrator dedicated for solving simultaneous sets of equations such as those represented by eq. (17) and eq. (18). For applications requiring very accurate solutions or where the computation time is not an issue, the moving pivot technique with even a black-box-type ODE integrator should be preferred. Of course, with a dedicated ODE integrator, the moving pivot technique will emerge to be a very powerful technique in terms of accuracy and the computation times.

4. CONCLUSIONS

We have shown in this work that the predictive capabilities of the macroscopic balances (or discretization techniques) for solving population balance equations can be significantly improved by accounting for variation of number density with size in a size range. This has been accomplished in a simple and approximate way (to guide the macroscopic balances to respond differently to two size ranges that contain same number of particles but distributed differently in size space) through the the location of a moving pivot that represents the total population of the corresponding size range.

Besides its additional qualities, the new moving pivot technique has the same general capabilities as the fixed pivot technique presented in Part I (Kumar and Ramkrishna, 1996), i.e. it can predict desired properties associated with an evolving size distribution by using a general grid (uniform, geometric or non-regular) for pure breakage, pure aggregation, polymerization–depolymerization (solution of discrete–continuous PBEs with simultaneous breakup and aggregation). It has therefore been evaluated here only for its additional features. A comparison of the numerical results for the fixed pivot (Part I) and the new technique (moving pivot) with the analytical results for the problems involving pure aggregation

indicates that the predictions with the new technique are indeed much closer to the analytical solutions. The new technique also serves to show that the correct discrete representation of the birth term due to coalescence of smaller drops (which determines the movement of the front) is crucial for the accuracy of the numerical solutions.

NOTATION

$\bar{B}_{i,t}^{(s)}$ as defined by eq. (12)

$\mathrm{CON}(v,t)$ number of particles of sizes greater than v at time t

$f_i(v)$ monotonically increasing functions of particle size v

$F_i(t)$ an integral property defined as $\int_0^\infty f_i(v)\, n(v,t)\,\mathrm{d}v$

$n(v,t)\,\mathrm{d}v$ number of particles in size range v to $v+\mathrm{d}v$, at time t

$g(v)$ a monotonically increasing function of particle size v

$N(t)$ total number of particles at time t

$N_i(t)$ total number of particles in ith size range at time t

$p(v)$ a monotonically increasing function particle size v

$\tilde{p}(v,t)$ a modified density defined as $p(v)n(v,t)$

$P_i(t)$ total estimate of density of density $\tilde{p}(v,t)$ for ith size range at time t, defined as $\int_{v_i}^{v_{i+1}} \tilde{p}(v,t)\,\mathrm{d}v$

$q(v,v')$ aggregation frequency

q_{x_i,x_j} aggregation frequency for sizes x_i, x_j, $q(x_i,x_j)$

r a parameter that defines the geometric grid of the type $v_{i+1}=rv_i$

$r(v,v')$ modified aggregation frequency, $[=q(v,v')/p(v)p(v')]$

r_{x_i,x_j} aggregation frequency for sizes x_i, x_j, $r(x_i,x_j)$

t time

$u(v)$ a monotonically increasing function of particle size v

v, v' particle volumes

v_i, v_{i+1} lower and upper boundaries for ith section

v_0 a parameter in eq. (20), equal to initial average volume

$x_i(t)$ representative volume for ith size range, function of time

Greek letters

$\beta(v,v')\,\mathrm{d}v$ number of daughter particles formed in size range v to $v+\mathrm{d}v$ due to the breakage of a particle of size v'

$\Gamma(v)$ breakage frequency for a particle size v

REFERENCES

Batterham, R. J., Hall, J. S. and Barton, G., 1981, Pelletizing kinetics and simulation of full scale balling circuits, *Proceedings of the 3rd International Symposium on Agglomeration.* Nurnberg, W. Germany, p. A136.

Bleck, R., 1970, A fast, approximate method for integrating the stochastic coalescence equation. *J. Geophys. Res.* **75**, 5165–5171.

Gelbard, F., Tambour, Y. and Seinfeld, J. H., 1980, Sectional representation of simulating aerosol dynamics. *J. Col. Interface Sci.* **76**, 541–556.

Hill, P. J. and Ng, K. M., 1995, New distribution procedure for the breakage equation. *A.I.Ch.E. J.* **41**, 1204–1216.

Hounslow, M. J., Ryall, R. L. and Marshall, V. R., 1988, A discretized population balance for nucleation, growth and aggregation. *A.I.Ch.E. J.* **34**, 1821–1832.

Kostoglou, M. and Karabelas, A. J., 1994, Evaluation of zero order methods for simulating particle coagulation. *J. Collid Interface Sci.* **163**, 420–431.

Kumar, S. and Ramkrishna, D., 1996, On the solution of population balance equations by discretization—I. A fixed pivot technique. *Chem. Engng Sci.* **51**, 1311–1332.

Litster, J. D., Smithi, D. J. and Hounslow, M. J., 1995, Adjustable discretized population balance for growth and Aggregation. *A.I.Ch.E. J.* **41**, 591–603.

Marchal, P., David, R., Klein, J. P. and Villermaux, J., 1988, Crystallization and precipitation engineering-I. An efficient method for solving population balances in crystallization with agglomeration, *Chem. Engng Sci.* **43**, 59–67.

Sastry, K. V. S. and Gaschignard, P., 1981, Discretization procedure for the coalescence equation of particulate processes. *IEC Fundam.* **20**, 355–361.

Scott, W. T., 1968, Analytical studies in cloud droplet coalescence-I. *J. Atmos. Sci.* **25**, 54–65.

Semino, D. and Ray, W. H., 1995, Control of systems described by population balance equations-I. Controllability analysis, II. Emulsion polymerization with constrained control action. *Chem. Engng Sci.* **50**, 1805–1839.